Published in final edited form as:
Structure. 2013 August 6; 21(8): 1307–1316. doi:10.1016/j.str.2013.06.018.

Inhibition versus potentiation of ligand-gated ion channels can be altered by a single mutation that moves ligands between intra- and inter-subunit sites

Torben Brömstrup[1,2], **Rebecca J. Howard**[3], **James R. Trudell**[4], **R. Adron Harris**[5], and **Erik Lindahl**[1,2,*]

[1]Science for Life Laboratory, KTH Royal Institute of Technology & Stockholm University, 17121 Solna, Sweden

[2]Center for Biomembrane Research, Department of Biochemistry & Biophysics, Stockholm University, 106 91 Stockholm, Sweden

[3]Department of Chemistry, Skidmore College, Saratoga Springs, NY, USA

[4]Department of Anesthesia and Beckman Program for Molecular and Genetic Medicine, Stanford University School of Medicine, Stanford, CA 94305

[5]Waggoner Center for Alcohol and Addiction Research, University of Texas at Austin, Austin, TX 78712

Abstract

Pentameric ligand-gated ion channels (pLGICs) are similar in structure but either inhibited or potentiated by alcohols and anesthetics. This dual modulation has previously not been understood, but the determination of X-ray structures of prokaryotic GLIC provides an ideal model system. Here, we show that a single-site mutation at the F14' site in the GLIC transmembrane domain turns desflurane and chloroform from inhibitors to potentiators, and that this is explained by competing allosteric sites. The F14'A mutation opens a new inter-subunit site lined by N239 (15'), I240 (16') and Y263. Free energy calculations confirm this site is the preferred binding location for desflurane and chloroform in GLIC F14'A. In contrast, both anesthetics prefer an intra-subunit site in wild-type GLIC. Modulation is therefore the net effect of competitive binding between the inter-subunit potentiating site and an intra-subunit inhibitory site. This provides direct evidence for a dual-site model of allosteric regulation of pLGICs.

Introduction

Despite their widespread use in surgery for over 150 years, the molecular action of volatile anesthetics is poorly understood. Early theories of nonspecific action on cell membranes have given way to evidence for direct modulation of membrane proteins, including the family of pentameric ligand-gated ion channels (pLGICs) (Miller, 2002; Urban and Bleckwenn, 2002). In this family, pharmacologically relevant concentrations of volatile anesthetics potentiate function of most $GABA_A$ receptors ($GABA_ARs$) and glycine

*erik.lindahl@scilifelab.se.

receptors (GlyRs), while they inhibit most nicotinic acetylcholine receptors (nAChRs) (Forman and Miller, 2011). The sites of action of volatile anesthetics on pLGICs are usually allosteric; they are believed to be distal to the site(s) of agonist binding, and for most channels it is not possible for the allosteric ligand to open the channel without the agonist present (Cascio, 2006). This remarkable diversity in the action of allosteric ligands in a single family of receptors is quite unique. It provides an interesting opportunity to better understand membrane protein conformational changes and allosteric modulation in general, as well as mechanisms of action for how volatile anesthetics and alcohol perturb the function of ligand-gated ion channels in particular. For a recent review, see e.g. (Corringer et al., 2012).

Since there are still no X-ray structures available for the $GABA_A$Rs and GlyRs, and only a lower-resolution cryo-EM structure exists for the nAChR (Unwin, 2005), some of the historically most important studies of pLGICs have used site-directed mutagenesis combined with photolabeling or electrophysiology to experimentally characterize the modulation sites for alcohols and anesthetics. Early photolabeling studies (Pedersen and Cohen, 1990) proposed a binding site between subunits for nAChRs, and more recent work has shown that the modulation of nAChR is influenced by a diverse range of binding sites, including a site in the extracellular domain (Ziebell et al., 2004) and two sites in the channel (Chiara et al., 2009; Pandhare et al., 2012) for charged ligands, while uncharged ligands might bind between subunits close to the extracellular end of M2 helix (Arevalo et al., 2005; Chiara et al., 2003). Time-resolved photolabeling studies have further identified state-dependent binding sites in the transmembrane (TM) domain and shown that agonist-driven channel opening can enhance anesthetic binding to a hydrophobic binding site, which could point to a selected fit model (Arevalo et al., 2005). There is also evidence for slow and fast desensitization of the channels being linked to separate conformational changes in two different cavities (Yamodo et al., 2010). Some of the first evidence for specific action sites of alcohol and volatile anesthetics on heteromeric GABA was provided by Mihic *et al.* (Mihic et al., 1997), using chimeric receptor constructs with α_1/β_2 subunits to identify α_1S270/β_2N265 (15' M2) and α_1A291/β_2M286 as critical for modulation.

Photolabeling studies on GABA with etomidate analogs (Chiara et al., 2012; Li et al., 2006) have identified inter-subunit binding of etomidate close to α_1S270/β_2N265 (M2 15'), and early simulations of homology models of GlyR could keep ethanol stable in an inter-subunit site formed by S267, A288 and I229 (Cheng et al., 2008). However, other data suggest the anesthetic propofol rather binds close to the extracellular end of the M3 segment in GABA, and, at least for GlyR, there are functional mutation studies indicating independent contributions of S267 (M2 15') and A52 in the extracellular domain loop 2 (Brejc et al., 2001), which suggests there might be multiple potentiating binding sites (Crawford et al., 2007; Mascia et al., 2000; Perkins et al., 2010).

As no high-resolution structure has yet been determined for a human pLGIC, substantial insight has emerged from the structures of closely related prokaryotic proteins such as the *Gloeobacter violaceus* ligand-gated ion channel (GLIC) (Bocquet et al., 2009; Hilf et al., 2010). This bacterial homolog shares 20% amino acid identity with the human α7 nAChR (Bocquet et al., 2007) and exhibits inhibition by volatile anesthetics, similar to nAChRs (Weng et al., 2010). GLIC has been an important template for homology models of human receptors, and in previous work we have reported microsecond simulations of GlyR where ethanol spontaneously diffuses to and binds in an inter-subunit location (Murail et al., 2011). This would appear to be contradicted by GLIC co-crystals with the anesthetics desflurane and propofol located in an intra-subunit site (Nury et al., 2011), but the recent structure of the eukaryotic GluCl channel by Hibbs *et al.* has the ligand ivermectin bound between subunits (Hibbs and Gouaux, 2011) in close contact with S260 (M2 15'), A261 and G262.

Superficially, all this data on different receptors might seem incompatible, although another option is the existence of multiple different binding sites for alcohols and/or anesthetics (Bali and Akabas, 2004; Ernst et al., 2005; Jansen and Akabas, 2006; Trudell and Bertaccini, 2004).

While the GLIC X-ray structures (Nury et al., 2011) point to a intra-subunit binding site, this prokaryotic channel is mostly inhibited by volatile anesthetics such as desflurane, propofol, or chloroform, as well as long chain n-alcohols in contrast to many of its eukaryotic homologs. This result makes it harder to say anything specific about the potentiating allosteric site and mechanism of pLGICs in general. However, recent mutagenesis studies of GLIC have opened new possibilities to use this channel as a model system for allosteric potentiation. Replacing the TM domain of GLIC by the α1 subunit from GlyR reverses modulation of GLIC by anesthetics and long-chain alcohols from inhibitory to potentiating (Duret et al., 2011), supporting this domain's role in mediating inhibition and potentiation. In fact, alcohols as large as *n*-hexanol can be converted from inhibitors to potentiators through a single point mutation, F238A, in the second TM helix (M2) of GLIC (Howard et al., 2011a). This mutation converts GLIC into a highly ethanol-sensitive channel comparable to its eukaryotic relatives GlyRs and GABA. Molecular dynamics (MD) simulations indicated this is caused by the opening of a new cavity at the inter-subunit interface that may mediate potentiation, without substantially altering the intra-subunit binding cavity observed in X-ray structures. We believe these changes cannot be explained from a single anesthetic or alcohol-binding site in pLGICs, no matter what the location is, but that it requires a dual action mechanism for channel inhibition and potentiation. Indeed, microsecond simulations of GLIC F238A in the presence of ethanol show enhanced inter-subunit density of ethanol (Murail et al., 2012), which would correlate well with the proposed binding sites for anesthetics and alcohols in eukaryotic channels (Bertaccini et al., 2005; Cheng et al., 2008; Forman and Miller, 2011).

Recent efforts to simulate anesthetic binding to GLIC using MD (Brannigan et al., 2010) or combined modeling and tryptophan quenching (Chen et al., 2010) have suggested binding to both intra-subunit and inter-subunit sites, as well as sites in the pore and in loop regions of TM domains. One approach to distinguish between such promiscuous possibilities is to calculate the free energies of binding of a computationally docked compound in various putative binding sites (Foloppe and Hubbard, 2006), an approach that is becoming increasingly accessible to membrane protein studies (Lebard et al., 2012; Lindahl and Sansom, 2008). In particular, quantitative data on the contributions of specific sites to anesthetic binding can be compared directly to experiments in order to connect functional and molecular-level data and critically test different models for modulation.

In this study, we provide evidence for a dual-site allosteric modulation effect on ligand-gated ion channels, where the intra-subunit site is inhibitory and the inter-subunit site potentiating. This has been achieved by combining electrophysiology with MD simulations to probe how the F238A mutation changes the modulation response of GLIC to volatile anesthetics. The single-site mutation not only shifts, but completely reverses the modulation effect in experiments, and causes GLIC to be potentiated rather than inhibited by desflurane and chloroform. By using docking to a range of putative sites as well as free energy calculations, we show this is explained by the presence of two binding sites, where the intra-subunit site has the best affinity for both compounds in wild-type (WT) GLIC, but in the F238A mutant the affinity is swapped with the anesthetics preferring inter-subunit binding. This provides direct support for an action model where desflurane and chloroform primarily bind intra-subunit in WT GLIC and inhibit the channel, while the F238A mutant has a potentiating binding site between subunits.

Results

GLIC WT and F238A channels are differentially modulated by volatile anesthetics

Whereas GLIC exhibits inhibition by long-chain alcohols such as *n*-hexanol, the single-site mutant F238A exhibits potentiation by the same agents (Howard et al., 2011a). Given past evidence that alcohols and volatile anesthetics may act via shared binding sites on pLGICs (Mascia et al., 2000), we investigated the modulation of GLIC by a variety of volatile anesthetics. We measured anesthetic modulation by two-electrode voltage clamp electrophysiology in *Xenopus laevis* oocytes of GLIC currents at 10 % maximal proton activation, using a similar protocol to that previously described for *n*-alcohols (Howard et al., 2011a). Pharmacologically relevant doses of volatile anesthetics are generally described by the minimum alveolar concentration (MAC) required to eliminate response to a noxious stimulus in 50% of subjects (Sonner et al., 2003). The volatile agents desflurane, chloroform, enflurane, and isoflurane inhibited the function of WT GLIC at or below 3 times MAC (Weng et al., 2010), while they potentiated the function of GLIC mutant F238A (Figure 1A).

To quantify the differential modulation of GLIC WT and F238A channels, we measured modulation at a range of concentrations of desflurane, an inhalational agent commonly used for general anesthesia (Meyer, 2010) that was recently co-crystallized in a TM intra-subunit site of GLIC (Nury et al., 2011). WT GLIC was inhibited by desflurane in a concentration-dependent manner with a half-maximal concentration (IC_{50}) of 1.1 mM, ~1.3 MAC ($LogIC_{50}$ −2.9 ± 0.087), and a Hill coefficient less than 1 (0.74 ± 0.19) (Figure 1B, black). Conversely, GLIC F238A exhibited little or no modulation up to 1 MAC desflurane, but was enhanced more than 4-fold by higher concentrations (Fig. 1B, orange). GLIC potentiation did not appear to saturate at the highest concentration tolerated by oocytes.

Structural details of intra-subunit and inter-subunit binding

To identify the binding differences between GLIC WT and F238A, we needed to find the best binding poses in the inter-subunit and intra-subunit cavities (Fig 2). We applied ligand docking to obtain initial binding sites followed by 20 ns unrestrained MD to identify multiple kinetically distinct binding poses. These poses were used to obtain binding affinities of both anesthetics in the two sites site of WT and F238A GLIC. The binding free energy was calculated independently for each pose, and an occupancy-weighted average calculated in each site. To increase sampling in the simulations, desflurane or chloroform ligands were placed in identical poses in each of the subunit sites (Fig. 2), although this is not strictly required for modulation in experiments (Mowrey et al., 2013).

Intra-subunit binding conformations

Desflurane was docked into GLIC WT and F238A by using the cavity from the experimentally identified binding site (Nury et al., 2011). Neither RMSD calculation nor manual inspection indicated any significant differences in the set of binding poses between the two structures (Fig. S1), which is reasonable since the mutation did not directly affect this site. The interaction site of desflurane in the docking-derived intra-subunit site was made up by I201, I202 and S205 (I206) of helix M1, V242 of M2, and T255, Y254, I258 (I259) of M3, which is identical to the interacting residues observed in the X-ray co-crystal reported earlier (Nury et al., 2011).

Representative conformations of desflurane obtained by clustering of snapshots along the trajectories, as well as visual inspection of the trajectories, indicated two poses (Fig. 3A). The conformational diversity and relatively high mobility of desflurane in the intra-subunit cavity (RMSF of 3.55 Å in WT and 2.96 Å in F238A) makes it difficult to compare with a

limited-resolution electron density. However, we found the representative conformation of one cluster to be within 0.6 Å RMSD of the crystal structure (Nury et al., 2011), which indicates some agreement between simulations and crystallographic data. The crystal structure points towards hydrogen bond formation between T255 and the oxygen atom of desflurane. However, while analysis of the trajectories shows that the mere distance between the oxygen of desflurane and the hydroxyl group of T255 might be compatible with hydrogen bonding, the geometric constraints for hydrogen bond formation are rarely fulfilled either in WT GLIC or the F238A mutant. The large mobility of desflurane suggests its binding in the intra-subunit site might not be due specifically to an h-bond between T255 and desflurane, but nonpolar interactions with I202, S205 and possibly polar interaction between desflurane and T255 (Figs. 3C, 3G) since T255A reduces inhibition (Nury et al., 2011). No differences in these local interactions were observed between WT and F238A simulations.

As the specific sub-site for binding chloroform intra-subunit is not known from crystallographic structures, we tested three different sub-sites. One location was found close to Y254 and T255 in M3 as well as I201 and S205 in M1 (Figs. 3D & 3E), which is identical to the binding site identified for desflurane. A second location involves I202 (M1) Y254 (M3) and N307 (M4), similar to the previously reported intra-subunit binding location for propofol (Nury et al., 2011). Finally, a third sub-site involves V242, F238/A238, N239 (M2) and Y263 (M3). The latter is closer to the linking tunnel between intra- and inter-subunit cavities, and less exposed to the hydrophobic membrane region. Despite the small size and high mobility (RMSF values up to 2.83 Å) of chloroform, it stayed completely within these pockets during a 20 ns unrestrained simulation. Chloroform assumes 3–4 different orientations that convert rapidly, and effectively behave as a single pose.

Inter-subunit binding conformations

The inter-subunit site is delimited by the M1, M2, M2’ and M3’ helices (with prime notation indicating the next subunit, Fig. 4). We started our initial simulations with different poses for desflurane and chloroform. The locations of these ranged from deep into the TM domain close to the 14’ site to poses at the EC-TM interface of the inter-subunit cavity. For WT GLIC and F238A, we investigated a binding site for desflurane close to the EC-TM interface (between N200 M1 and E243 M2’), similar to the site proposed for enflurane in GLIC (Chen et al., 2010). This part of the cavity is water-filled and made up by polar and charged residues N200, E243, K244, Y203, and S196 (Fig. 2 & Tab. S1). However, the binding free energies at this site turned out to be significantly higher than at the intersubunit sub-site close to the 14’ site. Further, we expected structural changes caused by the 14’ mutation to be minimal at this site and not cause significant changes in anesthetic binding. Therefore, we mainly investigated the binding poses in proximity of the 14’ site, close to the linking tunnel between the intra- and inter-subunit site (Figs. 4B & 4F). This is the only site where changes were large enough to potentially explain the inversion of the anesthetic effect.

The binding site was defined by M2 A238, I243; M1 I201, P204, I208; M2’ R239, I240, I236; M3’ 263 and lined by N200 and E243. The RMSF of desflurane bound to WT GLIC was 1.86 Å and for the F238A mutant 1.99 Å. Further, the two inter-subunit conformations of desflurane in WT GLIC occupied the same pocket with two kinetically distinct orientations that only rarely interconverted, while the MD trajectories of the poses in the F238A mutant showed fast interchange between several conformations. Desflurane binding in WT GLIC is located more towards the EC domain, with a mass center roughly at the level of I240. There is no overlap with the corresponding binding locations of desflurane in the F238A mutant, where the site is roughly at the height of I236. This difference was mainly explained by the steric restriction caused by the F238 phenyl ring in WT GLIC (cf. Figs. 4C, 4G), which also caused desflurane to bind closer to N200 and E243 in WT GLIC, where

there is a waterfilled polar cavity at the EC-TM interface. As a consequence, the ether group of desflurane is not able to form polar interactions with N239 and Y263 or hydrophobic interactions with I236 and Y263 further down in the cavity. In contrast, desflurane bound to GLIC F238A resulted in just a single cluster representing one binding pose, where the ligand has characteristic polar interactions with M2' N239 and M3' Y263 and hydrophobic interactions with M3' 263; M2' I236 and M2 A238.

For chloroform in the inter-subunit cavity, we identified a single site in WT GLIC with four slightly different conformations. As for desflurane, chloroform in the WT structure did not penetrate deeper than the level of I240 (16') in M2', which is significantly above the 14' site. Three of the conformations identified were close to this 16' site where they interact with N239 of M2' (15'), and the last conformation close to N200 and E243 (similar to the desflurane binding in WT, Fig. 4D). For chloroform too, there was a marked change of binding properties with the mutation. Chloroform binding to F238A GLIC had two kinetically distinct poses; the first is below the 14' site close to I236 (M2'), A238 (M2) and the aromatic ring of Y263 (M3'), while the second pose is one helix turn further up at 16' (I240 in M2'), forming polar contacts to N239 and Y263.

Binding Free Energies

The free energy of binding in each site was derived from MD simulations where ligands were restrained in each kinetically distinct orientation and interactions gradually decoupled (Wang et al., 2006). The free energy of binding for desflurane in the GLIC WT intra-subunit cavity was −21.8 ± 0.3 kJ/mol compared to −19.7 ± 0.4 kJ/mol for F238A (Fig. 5). Importantly, these standard error estimates only refer to the ligand sampling, not the much slower relaxation of the protein, which means the difference is likely not significant. For the intra-subunit binding of chloroform, we calculated free energies in three different pockets. For the deeply buried pocket at the 14' site close to V242, N239, and Y263, we retrieved a binding free energy of −3.9 ± 0.4 kJ/mol for WT and −4.1 ± 0.4 kJ/mol for the mutant. The chloroform sites that most closely resembled the propofol binding sites had binding free energies of −14.6 ± 0.3 kJ/mol for WT and −13.9 ± 0.4 kJ/mol for F238A. The intra-subunit chloroform site showing the strongest binding resulted in free energies of −18.6 ± 0.4 kJ/mol for WT and −15.5 ± 0.1 kJ/mol for F238A, which is closer to the binding affinity of desflurane. This reduction in affinity was not coupled to any change of pose, and further analysis indicated it is rather due to increased water penetration into the intra-subunit site, which as discussed previously by Howard *et al.* (Howard et al., 2011a) is a result of the increased volume of the inter-subunit site in GLIC F238A (Tab. S1).

For binding between subunits, we first considered the higher-level site located closer to the EC domain. For desflurane binding in WT GLIC, the binding energy in this site was only −9.5 ± 0.4 kJ/mol, which was the worst of all scanned sites. Since this location is also relatively far from the 14' site, we did not expect large changes from the F238A mutation, and decided not to pursue this site further. To evaluate binding in the lower-level cavity (closer to 14'), the overall free energy of binding was obtained from occupancy-weighted averaging of the free energies of the multiple kinetically distinct poses. At the inter-subunit 14' site the total free energy of desflurane binding was −14.4 ± 0.6 kJ/mol for WT GLIC and −23.2 ± 0.5 kJ/mol for the F238A mutant. Similarly, for chloroform the free energy of binding in the inter-subunit site was 16.2 ± 0.6 kJ/mol and −24.8 ± 0.3 kJ/mol for WT and F238A, respectively. Some caution is advised since protein relaxation could affect these values on longer timescales, although we do not expect binding to *deteriorate* in the mutant with relaxation (which would be required to alter the qualitative result). The shifts in the inter-subunit site are close to 10 kJ/mol, and even a relative difference of 5 kJ/mol corresponds to a factor ~10 in occupancy at room temperature. In other words, this suggests the intra-subunit site is heavily favored for desflurane and favored for chloroform in WT

GLIC, whereas the F238A mutation clearly shifts the most favorable location to the inter-subunit site for both ligands (Tab. S2).

To test cooperativity between the two binding sites in F238A, we also calculated the free energies when desflurane was present in both binding sites. For the intra-subunit binding of desflurane, where desflurane was also present in the inter-subunit, we obtain −20.9 ± 0.8 kJ/mol compared to −19.7 ± 0.4 kJ/mol without the extra ligand. The inter-subunit site binding of desflurane with desflurane also present in the intra-subunit site was −23.9 ± 0.3 compared to −23.2 ± 0.5 kJ/mol for the reference case. Thus, it appears prior binding in one site has little influence on the affinity in the other site.

Discussion

We previously showed that GLIC exhibits bimodal modulation by *n*-alcohols, being potentiated by short-chain alcohols (methanol, ethanol) but inhibited by long-chain alcohols (propanol and larger) (Howard et al., 2011a). Substituting alanine for phenylalanine at the 14’ position in the GLIC M2 helix (F238A) dramatically altered alcohol modulation, enhancing potentiation by short-chain alcohols and converting alcohols as large as *n*-hexanol from inhibitors into potentiators (Howard et al., 2011a). The present work now shows that the F238A mutation also completely reverses the action of several volatile anesthetics, converting them from inhibitors into potentiators. Thus, consistent with past evidence that alcohols and anesthetics act via shared binding sites on pLGICs (Mascia et al., 2000), long-chain *n*-alcohols and anesthetics modulate GLIC in a parallel fashion, involving the F238 residue. Our free energy calculations on docked desflurane and chloroform suggest this is coupled to differential binding, with the intra-subunit site being preferred in wild-type GLIC, while the inter-subunit site is enlarged and favored in the F238A mutant. We propose a model with two sites of action with opposing effects. The functional effect on the channel is a result of competitive binding between these two sites, although there does not appear to be any cooperativity effects between the sites. This could explain the complex dose-response curve where binding to a single site initially causes the effect, but when this is saturated and the second site is increasingly occupied, the effect is suddenly reversed. In contrast, a single site-model where occupancy triggers different modes of action would likely result in a linear dose-response curve.

Previous structural studies raised the possibility that the occupancy of anesthetics, even at saturating concentrations, might be low in GLIC TM cavities, given the high B-factors associated with the bound drugs (Nury et al., 2011). In contrast, our simulations are consistent with the explanation that high B-factors arise from high mobility and conformational entropy of the anesthetic molecule within its binding site: in many cases, the modulator was seen to flip its orientation 180° several times in the course of a single simulation. We were able to observe this mobility in all five semi-symmetric cavities docked in each simulation, but with no evident cooperativity. This high mobility may arise from a lack of strong electrostatic interactions defining a particular pose in the binding cavity.

Assuming high overall occupancy, we infer that even relatively disfavored binding sites contribute to the net modulation, particularly under the high (low-mM) concentrations of anesthetics used for functional experiments in this study. This hypothesis is consistent with previous studies supporting the existence of multiple simultaneous interaction sites for allosteric modulators on pLGICs, in some cases with opposing functional consequences (Borghese et al., 2003; Crawford et al., 2007; Howard et al., 2011b). Indeed, the low Hill coefficients observed for anesthetic inhibition of WT GLIC is consistent with multiple antagonistic sites of action, or possibly with negative cooperativity (Weng et al., 2010). We also noted that, although high concentrations of desflurane dramatically potentiated GLIC

F238A currents, moderate concentrations (< 3 MAC) had a smaller absolute effect on the mutant than on WT: 1 MAC desflurane inhibited WT GLIC by 50 %, but did not significantly alter GLIC F238A. This decreased apparent affinity is consistent with more closely balanced binding at opposing sites of action in the mutant, as predicted by our binding free energy calculations.

The intra-subunit cavity used for initial docking in this study was the unique site of desflurane binding in a recent crystal structure of WT GLIC (Nury et al., 2011). Of the three binding poses we identified for desflurane in WT GLIC, the highest-affinity one was remarkably close to the X-ray co-crystal. Chloroform too was found to bind in this location, while the propofol site in the co-crystal is more similar to one of our alternative poses. Given that WT GLIC exhibits net inhibition by desflurane, this site was proposed to be an inhibitory site of action (Nury et al., 2011). Conversely, a nearby cavity at the inter-subunit interface was recently implicated in potentiating actions of *n*-alcohols on GLIC (Howard et al., 2011a) as well as GlyRs (Murail et al., 2011). In this study, we provide quantitative measures of the relative free energies of binding to the intra-subunit (putative inhibitory) and inter-subunit (putative potentiating) cavities in GLIC WT and F238A channels. The F238A mutation made desflurane binding to the intra-subunit site slightly less favorable, but enhanced binding to the inter-subunit site two-fold. The net effect implies there should be an inversion of the occupancy in the two sites, which correlates well with a switch from inhibition to potentiation by desflurane.

In the inter-subunit cavity, we tested three possible docking poses at varying levels of penetration into the TM core. For the F238A mutant, the deepest binding pose—essentially occupying the cavity left by the substituted F238 side chain—was the most favorable. However, in the WT protein, this pose was almost completely occluded; instead, the optimal inter-subunit pose was translated by one helical turn towards the extracellular medium, near residue L241. This binding pose is supported by our previous demonstration that small substitutions at residue 241 enhance ethanol potentiation, and that labeling of this residue with a small methanethiosulfonate reagent mimics alcohol potentiation (Howard et al., 2011a). We tested an additional binding pose even further towards the extracellular space, but found it to be a less significant contributor to binding in either WT or mutant proteins.

The free energy calculations also indicate that desflurane binds with similar affinity to the intra-subunit and inter-subunit cavities of the GLIC F238A mutant. Indeed, as discussed above, moderate desflurane concentrations (1 MAC) have no net effect on GLIC F238A, possibly reflecting a balance of inhibiting and potentiating actions. Although one cannot directly translate affinity to efficacy, this might be reflected in the free energies where the difference between the two sites in F238A is much smaller for desflurane (one in four desfluranes would still occupy the inhibitory site) than chloroform (one in 50).

However, at high concentrations, desflurane is a strong potentiator of the GLIC F238A mutant. The net functional effect, then, may arise from a combination of inhibitory binding to the intra-subunit cavity, plus potentiating interactions with the inter-subunit cavity that are of higher absolute efficacy. As the putative inhibitory effect of binding in the intra-subunit cavity saturates, binding to an inter-subunit site with a relatively higher efficacy (but for potentiation rather than inhibition) could yield the strong net enhancement observed experimentally. This is in agreement with a multiple-site model for allosteric regulation. In the WT channel, the low affinity of binding in the inter-subunit cavity may render it a negligible contributor to net modulation, except at very high concentrations not tolerated in our oocyte assay. Of course, it is also possible that structural changes brought by the F238A mutation increase the efficacy of inter-subunit binding relative to WT, such that the

increased affinity reflected in our free energy calculations leads to an even more dramatically increased potency of potentiation at high concentrations.

In addition to the intra-subunit and inter-subunit TM cavities studied here, previous molecular dynamics studies (Brannigan et al., 2010; Chen et al., 2010) have implicated anesthetic binding sites near the channel pore and M2–M3 loop. Although our simulations provide a simple quantitative basis for our functional observations, there could be possible contributions from additional binding sites or possibly competitive effects from pore blocking (Lebard et al., 2012); some of this might be possible to test by combining free energy calculations of the two sites studied here with pore blocking to understand pLGIC modulation, although this might require an extension to the simplified two-site model. However, given the presumed promiscuity of anesthetic binding, and their evidently high mobility within a given binding site, we defined the “intra-subunit” and “inter-subunit” site for each protein as the most favorable of a variety of tested poses. Docking of desflurane in the intra-subunit cavity yielded a binding pose superimposable with that observed in the crystal structure (Nury et al., 2011). Docking in alternative poses in this WT cavity yielded less favorable energies. Furthermore, the intra-subunit binding pose observed for WT GLIC was conserved in the F238A structure, consistent with the comparable free energy of intra-subunit binding for the two proteins.

The binding of general anesthetics to GLIC is likely not limited to the intra-subunit (I202, S205, T255) and the inter-subunit (N239, Y263, I236) sites. A binding site close to the TMD/ECD interface reported for halothane and thiopental above N200 (Chen et al., 2010) might also be suitable for polar anesthetics. Despite lower affinity, we too observed a possible binding pose for desflurane in this location in WT GLIC, and ethanol modulation of GLIC was also somewhat affected by alterations to I240, L241, or N245.

Phenylalanine is conserved at the M2 14’ position of several subtypes of nAChRs, which—like GLIC—were previously shown to exhibit potentiation by short-chain alcohols but inhibition by anesthetics and long-chain alcohols (Borghese et al., 2003). Conversely, the equivalent residue is generally smaller and more polar in channels such as $GABA_A$Rs and GlyRs, which exhibit potentiation rather than inhibition by anesthetics and alcohols. The recently crystallized GluClα has a glutamine in this position, and the co-crystal with the potentiator Ivermectin shows the large ligand to be placed between subunits (Hibbs and Gouaux, 2011), overlapping with our highest-affinity site for anesthetics in GLIC F238A. The effect of substituting a smaller, more polar residue at the 14’ position in GLIC is thus consistent with a role for this position, and the nearby inter-subunit cavity, in differential sensitivity of pLGICs to allosteric modulators. Previous studies on GlyR and $GABA_A$R linked several residues belonging to different subunits to the modulation of anesthetics and alcohols, which supports functional effects between subunits, in particular the 15’ residues α_1S270/β_2N265 (15’ M2) of $GABA_A$R (Mihic et al., 1997) and S267 (15’ M2) of GlyR or S260 (15’ M2) of GluCl (Cheng et al., 2008). These sites are very close to the 14’ site in the present study and support a general anesthetic-and alcohol-binding site in this location, which appears to be confirmed by a recent GLIC F238A co-crystal with ethanol bound inter-subunit (Sauguet et al., 2013). Similarly, the earlier structure of GLIC in a locally closed state (Prevost et al., 2012) indicates that the extracellular part of M2 helix has moved inwards, to some extent detached from M3, and opened a cavity between them. Our intra-subunit site is located close to the lower part of this cavity, and it appears quite reasonable that ligand-binding in this site could stabilize an already-closed channel, resulting in the observed inhibition, while potentiation in GLIC F238A might be caused by subunits not being able to move inwards when ligands are bound between them.

In addition to the binding interactions studied here, there may be indirect effects of the F238A mutation on modulation due to changes in the energetics of gating. As described previously, the mutation did right-shift the proton concentration dependence, adjusting the 10 % activation condition from pH 5.5 to pH 5.0; however, neighboring mutations that elicited similar shifts in gating (e.g. A237C, N239C) did not evoke similar changes in alcohol modulation, suggesting that these effects were independent (Howard et al., 2011a). It should also be noted that our structural models are based on the crystallographic, presumed open (Bocquet et al., 2009; Hilf et al., 2010) or desensitized (Gonzalez-Gutierrez and Grosman, 2010; Parikh et al., 2011) state of GLIC. The pore radius did not change significantly during the short timescale of our simulations (Fig. S2), which is not suprising since closing, desensitizing, or opening are likely much slower transitions. A complete understanding of the impact of modulator binding in the sites studied here or elsewhere will require a detailed model of the channel's opening and closing transitions, including the relative free energies of the channel in (future) closed vs. open states and the transition states between them. However, better understanding of anesthetic binding in the inter-subunit site is a first important step towards understanding modulation of ligand-gated channels in general.

Materials and Methods

Experimental Materials

Volatile anesthetics were purchased from Marsam Pharmaceuticals Inc. (Cherry Hill, NJ); all other chemicals were purchased from Sigma-Aldrich (St. Louis, MO). Expression plasmids containing GLIC WT and F238A cDNA in the PMT3 vector were prepared as previously described (Howard et al., 2011a). The oocytes were prepared from ovarian tissue of *Xenopus laevis* frogs for the two-electrode voltage clamp electrophysiology. GLIC currents were measured for pH-dependent GLIC activation as previously described (Howard et al., 2011a) (see supplemental information for additional details).

Volatile anesthetic solutions were adjusted to deliver the reported concentration calibrated by gas chromatography, as described previously (Lin et al., 1992). The adjusted anesthetic volume was added via positive displacement pipette to the appropriate Ringer's buffer in a scintillation vial with minimal head space, immediately sealed with parafilm and aluminum foil, and sonicated for ≥ 2 min. The solution was applied by piercing the seal with the perfusion input needle, minimizing exposure of the solution surface to atmosphere. To quantify anesthetic modulation, oocytes were treated for 1 min with low-pH Ringer's buffer; after 5 min washout, the anesthetic solution was applied in neutral Ringer's buffer for 1 min, then in low-pH buffer for 1 min; after another 5 min washout, low-pH buffer was again applied alone. Modulation was calculated as $[(R_A - \langle R_0,R_1\rangle) / \langle R_0,R_1\rangle] \times 100$, where R_A represents the channel response in the presence of anesthetic and $\langle R_0,R_1\rangle$ represents the mean of the pre-and post-anesthetic responses. Initial anesthetic concentrations were chosen as 3 times MAC, except for chloroform, for which ~1 MAC was used on account of the large degree of modulation. Values of MAC were derived as previously described (Mihic et al., 1994).

Statistics

Data are represented as mean ± s.e.m. Results were analyzed by two-tailed unpaired *t* test with significant effects set at $p < 0.05$. The desflurane inhibition curve for wild-type GLIC was calculated by nonlinear regression fit to the equation M = 100 / (1 + 10 ^ [log(IC_{50} − A)] · n_H) − 100, where M is the % modulation, A is the molar concentration of desflurane, IC_{50} is the concentration producing 50 % inhibition, and n_H is the Hill coefficient. Nonlinear

regression analysis and all statistical analyses were performed with GraphPad Prism 5 for Mac (GraphPad Software, San Diego, CA).

Molecular Modeling

Protein data bank entry 3EAM (Bocquet et al., 2009) was used for WT GLIC. Both WT and F238A systems were embedded into a DOPC bilayer, solvated and set to 100 mM concentration of NaCl (Howard et al., 2011a). Both systems were subject to 20 ns of simulation with position restraints on backbone atoms, and the mutant relaxed another 200 ns. Initial ligand poses were identified with AutoDock 4.2 (Morris et al., 1998) and subject to 20 ns unrestrained simulations with GROMACS (Hess et al., 2008) to get the kinetically distinct ligand binding poses. A restraining potential was used during free energy calculations (Fig. S3). Additional details about docking and parameters are described in the supplemental information.

Supplementary Material

Refer to Web version on PubMed Central for supplementary material.

Acknowledgments

This work was supported by the European Research Council (209825), the Foundation for Strategic Research, the Swedish Research Council (2010-491,2010-5107), the Swedish e-Science Research Center, National Institutes of Health/National Institutes on Alcohol Abuse and Alcoholism Grants T32 AA007471, R01 AA06399, and R01 AA013378. Computational resources were provided by the Swedish National Infrastructure for Computing.

Bibliography

Arevalo E, Chiara DC, Forman SA, Cohen JB, Miller KW. Gating-enhanced accessibility of hydrophobic sites within the transmembrane region of the nicotinic acetylcholine receptor's {delta}-subunit. A time-resolved photolabeling study. J Biol Chem. 2005; 280:13631–13640. [PubMed: 15664985]

Bali M, Akabas MH. Defining the propofol binding site location on the GABAA receptor. Mol Pharmacol. 2004; 65:68–76. [PubMed: 14722238]

Bertaccini EJ, Shapiro J, Brutlag DL, Trudell JR. Homology modeling of a human glycine alpha 1 receptor reveals a plausible anesthetic binding site. J Chem Inf Model. 2005; 45:128–135. [PubMed: 15667138]

Bocquet N, de Carvalho LP, Cartaud J, Neyton J, Le Poupon C, Taly A, Grutter T, Changeux JP, Corringer PJ. A prokaryotic proton-gated ion channel from the nicotinic acetylcholine receptor family. Nature. 2007; 445:116–119. [PubMed: 17167423]

Bocquet N, Nury H, Baaden M, Le Poupon C, Changeux JP, Delarue M, Corringer PJ. X-ray structure of a pentameric ligand-gated ion channel in an apparently open conformation. Nature. 2009; 457:111–114. [PubMed: 18987633]

Borghese CM, Henderson LA, Bleck V, Trudell JR, Harris RA. Sites of excitatory and inhibitory actions of alcohols on neuronal alpha 2 beta 4 nicotinic acetylcholine receptors. J Pharmacol Exp Ther. 2003; 307:42–52. [PubMed: 14500778]

Brannigan G, LeBard DN, Henin J, Eckenhoff RG, Klein ML. Multiple binding sites for the general anesthetic isoflurane identified in the nicotinic acetylcholine receptor transmembrane domain. P Natl Acad Sci USA. 2010; 107:14122–14127.

Brejc K, van Dijk WJ, Klaassen RV, Schuurmans M, van Der Oost J, Smit AB, Sixma TK. Crystal structure of an ACh-binding protein reveals the ligand-binding domain of nicotinic receptors. Nature. 2001; 411:269–276. [PubMed: 11357122]

Cascio M. Modulating inhibitory ligand-gated ion channels. AAPS J. 2006; 8:E353–E361. [PubMed: 16796386]

Chen Q, Cheng MH, Xu Y, Tang P. Anesthetic binding in a pentameric ligand-gated ion channel: GLIC. Biophys J. 2010; 99:1801–1809. [PubMed: 20858424]

Cheng MH, Coalson RD, Cascio M. Molecular dynamics simulations of ethanol binding to the transmembrane domain of the glycine receptor: implications for the channel potentiation mechanism. Proteins. 2008; 71:972–981. [PubMed: 18004757]

Chiara DC, Dangott LJ, Eckenhoff RG, Cohen JB. Identification of nicotinic acetylcholine receptor amino acids photolabeled by the volatile anesthetic halothane. Biochemistry. 2003; 42:13457–13467. [PubMed: 14621991]

Chiara DC, Dostalova Z, Jayakar SS, Zhou X, Miller KW, Cohen JB. Mapping general anesthetic binding site(s) in human alpha1beta3 gamma-aminobutyric acid type A receptors with [(3)H]TDBzl-etomidate, a photoreactive etomidate analogue. Biochemistry. 2012; 51:836–847. [PubMed: 22243422]

Chiara DC, Hamouda AK, Ziebell MR, Mejia LA, Garcia G 3rd, Cohen JB. [(3)H]chlorpromazine photolabeling of the torpedo nicotinic acetylcholine receptor identifies two state-dependent binding sites in the ion channel. Biochemistry. 2009; 48:10066–10077. [PubMed: 19754159]

Corringer PJ, Poitevin F, Prevost MS, Sauguet L, Delarue M, Changeux JP. Structure and pharmacology of pentameric receptor channels: from bacteria to brain. Structure. 2012; 20:941–956. [PubMed: 22681900]

Crawford DK, Trudell JR, Bertaccini EJ, Li KX, Davies DL, Alkana RL. Evidence that ethanol acts on a target in Loop 2 of the extracellular domain of alpha 1 glycine receptors. J Neurochem. 2007; 102:2097–2109. [PubMed: 17561937]

Duret G, Van Renterghem C, Weng Y, Prevost M, Moraga-Cid G, Huon C, Sonner JM, Corringer PJ. Functional prokaryotic-eukaryotic chimera from the pentameric ligand-gated ion channel family. P Natl Acad Sci USA. 2011; 108:12143–12148.

Ernst M, Bruckner S, Boresch S, Sieghart W. Comparative models of GABAA receptor extracellular and transmembrane domains: important insights in pharmacology and function. Mol Pharmacol. 2005; 68:1291–1300. [PubMed: 16103045]

Foloppe N, Hubbard R. Towards predictive ligand design with free-energy based computational methods? Curr Med Chem. 2006; 13:3583–3608. [PubMed: 17168725]

Forman SA, Miller KW. Anesthetic sites and allosteric mechanisms of action on Cys-loop ligand-gated ion channels. Can. J. Anaesth. 2011; 58:191–205. [PubMed: 21213095]

Gonzalez-Gutierrez G, Grosman C. Bridging the gap between structural models of Nicotinic Receptor superfamily Ion Channels and their corresponding functional states. J. Mol. Biol. 2010; 403:693–705. [PubMed: 20863833]

Hess B, Kutzner C, van der Spoel D, Lindahl E. GROMACS 4: Algorithms for highly efficient, load-balanced, and scalable molecular simulation. J. Chem. Theory Comput. 2008; 4:435–447.

Hibbs RE, Gouaux E. Principles of activation and permeation in an anion-selective Cys-loop receptor. Nature. 2011; 474:54–60. [PubMed: 21572436]

Hilf RJ, Bertozzi C, Zimmermann I, Reiter A, Trauner D, Dutzler R. Structural basis of open channel block in a prokaryotic pentameric ligand-gated ion channel. Nat Struct Mol Biol. 2010; 17:1330–1336. [PubMed: 21037567]

Howard RJ, Murail S, Ondricek KE, Corringer PJ, Lindahl E, Trudell JR, Harris RA. Structural basis for alcohol modulation of a pentameric ligand-gated ion channel. Proc Natl Acad Sci U S A. 2011a; 108:12149–12154. [PubMed: 21730162]

Howard RJ, Slesinger PA, Davies DL, Das J, Trudell JR, Harris RA. Alcohol-binding sites in distinct brain proteins: the quest for atomic level resolution. Alcohol. Clin. Exp. Res. 2011b; 35:1561–1573. [PubMed: 21676006]

Jansen M, Akabas MH. State-dependent cross-linking of the M2 and M3 segments: Functional basis for the alignment of GABA(A) and acetylcholine receptor M3 segments. J. Neurosci. 2006; 26:4492–4499. [PubMed: 16641228]

Laskowski RA. SURFNET: a program for visualizing molecular surfaces, cavities, and intermolecular interactions. J. Mol. Graph. 1995; 13:323–330. 307–328. [PubMed: 8603061]

Lebard DN, Henin J, Eckenhoff RG, Klein ML, Brannigan G. General anesthetics predicted to block the GLIC pore with micromolar affinity. PLoS Comput Biol. 2012; 8:e1002532. [PubMed: 22693438]

Li GD, Chiara DC, Sawyer GW, Husain SS, Olsen RW, Cohen JB. Identification of a GABA(A) receptor anesthetic binding site at subunit interfaces by photolabeling with an etomidate analog. J. Neurosci. 2006; 26:11599–11605. [PubMed: 17093081]

Lin LH, Chen LL, Zirrolli JA, Harris RA. General anesthetics potentiate gamma-aminobutyric acid actions on gamma-aminobutyric acidA receptors expressed by Xenopus oocytes: lack of involvement of intracellular calcium. J Pharmacol Exp Ther. 1992; 263:569–578. [PubMed: 1331405]

Lindahl E, Sansom MS. Membrane proteins: molecular dynamics simulations. Curr Opin Struct Biol. 2008; 18:425–431. [PubMed: 18406600]

Mascia MP, Trudell JR, Harris RA. Specific binding sites for alcohols and anesthetics on ligand-gated ion channels. P Natl Acad Sci USA. 2000; 97:9305–9310.

Meyer T. Managing inhaled anesthesia: Challenges from a health-system pharmacist's perspective. Am J Health-Syst Ph. 2010; 67:S4–S8.

Mihic SJ, McQuilkin SJ, Eger EI 2nd, Ionescu P, Harris RA. Potentiation of gamma-aminobutyric acid type A receptor-mediated chloride currents by novel halogenated compounds correlates with their abilities to induce general anesthesia. Mol Pharmacol. 1994; 46:851–857. [PubMed: 7969071]

Mihic SJ, Ye Q, Wick MJ, Koltchine VV, Krasowski MD, Finn SE, Mascia MP, Valenzuela CF, Hanson KK, Greenblatt EP, et al. Sites of alcohol and volatile anaesthetic action on GABA(A) and glycine receptors. Nature. 1997; 389:385–389. [PubMed: 9311780]

Miller KW. The nature of sites of general anaesthetic action. Br J Anaesth. 2002; 89:17–31. [PubMed: 12173229]

Morris GM, Goodsell DS, Halliday RS, Huey R, Hart WE, Belew RK, Olson AJ. Automated docking using a Lamarckian genetic algorithm and an empirical binding free energy function. J. Comput. Chem. 1998; 19:1639–1662.

Mowrey D, Cheng MH, Liu LT, Willenbring D, Lu X, Wymore T, Xu Y, Tang P. Asymmetric ligand binding facilitates conformational transitions in pentameric ligand-gated ion channels. J. Am. Chem. Soc. 2013

Murail S, Broemstrup T, Howard RJ, Bertaccini E, Harris RA, Trudell J, Lindahl E. Molecular mechanism for the dual alcohol modulation of Cys-loop receptors. PLoS Comput Biol. 2012; 8:e1002710. [PubMed: 23055913]

Murail S, Wallner B, Trudell JR, Bertaccini E, Lindahl E. Microsecond simulations indicate that ethanol binds between subunits and could stabilize an open-state model of a glycine receptor. Biophys J. 2011; 100:1642–1650. [PubMed: 21463577]

Nury H, Van Renterghem C, Weng Y, Tran A, Baaden M, Dufresne V, Changeux JP, Sonner JM, Delarue M, Corringer PJ. X-ray structures of general anaesthetics bound to a pentameric ligand-gated ion channel. Nature. 2011; 469:428–431. [PubMed: 21248852]

Pandhare A, Hamouda AK, Staggs B, Aggarwal S, Duddempudi PK, Lever JR, Lapinsky DJ, Jansen M, Cohen JB, Blanton MP. Bupropion binds to two sites in the Torpedo nicotinic acetylcholine receptor transmembrane domain: a photoaffinity labeling study with the bupropion analogue [(125)I]-SADU-3-72. Biochemistry. 2012; 51:2425–2435. [PubMed: 22394379]

Parikh RB, Bali M, Akabas MH. Structure of the M2 transmembrane segment of GLIC, a prokaryotic Cys loop receptor homologue from Gloeobacter violaceus, probed by substituted cysteine accessibility. J Biol Chem. 2011; 286:14098–14109. [PubMed: 21362624]

Pedersen SE, Cohen JB. d-Tubocurarine binding sites are located at alpha-gamma and alpha-delta subunit interfaces of the nicotinic acetylcholine receptor. Proc Natl Acad Sci U S A. 1990; 87:2785–2789. [PubMed: 2320589]

Perkins DI, Trudell JR, Crawford DK, Alkana RL, Davies DL. Molecular targets and mechanisms for ethanol action in glycine receptors. Pharmacology & therapeutics. 2010; 127:53–65. [PubMed: 20399807]

Pettersen EF, Goddard TD, Huang CC, Couch GS, Greenblatt DM, Meng EC, Ferrin TE. UCSF chimera - A visualization system for exploratory research and analysis. J. Comput. Chem. 2004; 25:1605–1612. [PubMed: 15264254]

Prevost M, Sauguet L, Nury H, Van Renterghem C, Huon C, Poitevin F, Baaden M, Delarue M, Corringer PJ. A locally closed conformation of a bacterial pentameric proton-gated ion channel. Nat Struct Mol Biol. 2012; 19:642–649. [PubMed: 22580559]

Sauguet L, Howard RJ, Malherbe L, Lee US, Corringer PJ, Harris RA, Delarue M. Structural basis for potentiation by alcohols and anaesthetics in a ligand-gated ion channel. Nature Comm. 2013; 4:1697.

Sonner JM, Antognini JF, Dutton RC, Flood P, Gray AT, Harris RA, Homanics GE, Kendig J, Orser B, Raines DE, et al. Inhaled anesthetics and immobility: Mechanisms, mysteries, and minimum alveolar anesthetic concentration. Anesth Analg. 2003; 97:718–740. [PubMed: 12933393]

Trudell JR, Bertaccini E. Comparative modeling of a GABAA alpha1 receptor using three crystal structures as templates. J. Mol. Graph. Model. 2004; 23:39–49. [PubMed: 15331052]

Unwin N. Refined structure of the nicotinic acetylcholine receptor at 4A resolution. J. Mol. Biol. 2005; 346:967–989. [PubMed: 15701510]

Urban BW, Bleckwenn M. Concepts and correlations relevant to general anaesthesia. Br J Anaesth. 2002; 89:3–16. [PubMed: 12173238]

Wang J, Deng Y, Roux B. Absolute binding free energy calculations using molecular dynamics simulations with restraining potentials. Biophys J. 2006; 91:2798–2814. [PubMed: 16844742]

Weng Y, Yang LY, Corringer PJ, Sonner JM. Anesthetic sensitivity of the Gloeobacter violaceus Proton-Gated Ion Channel. Anesth Analg. 2010; 110:59–63. [PubMed: 19933531]

Yamodo IH, Chiara DC, Cohen JB, Miller KW. Conformational changes in the nicotinic acetylcholine receptor during gating and desensitization. Biochemistry. 2010; 49:156–165. [PubMed: 19961216]

Ziebell MR, Nirthanan S, Husain SS, Miller KW, Cohen JB. Identification of binding sites in the nicotinic acetylcholine receptor for [3H]azietomidate, a photoactivatable general anesthetic. J Biol Chem. 2004; 279:17640–17649. [PubMed: 14761946]

Highlights

- Desflurane and chloroform inhibits wild-type ligand-gated ion channels like GLIC
- This is coupled to an intra-subunit site having highest affinity for WT GLIC
- A single-site mutation F238A reverses action and turns the ligands into potentiators
- This is explained by a new inter-subunit site with even higher binding affinity

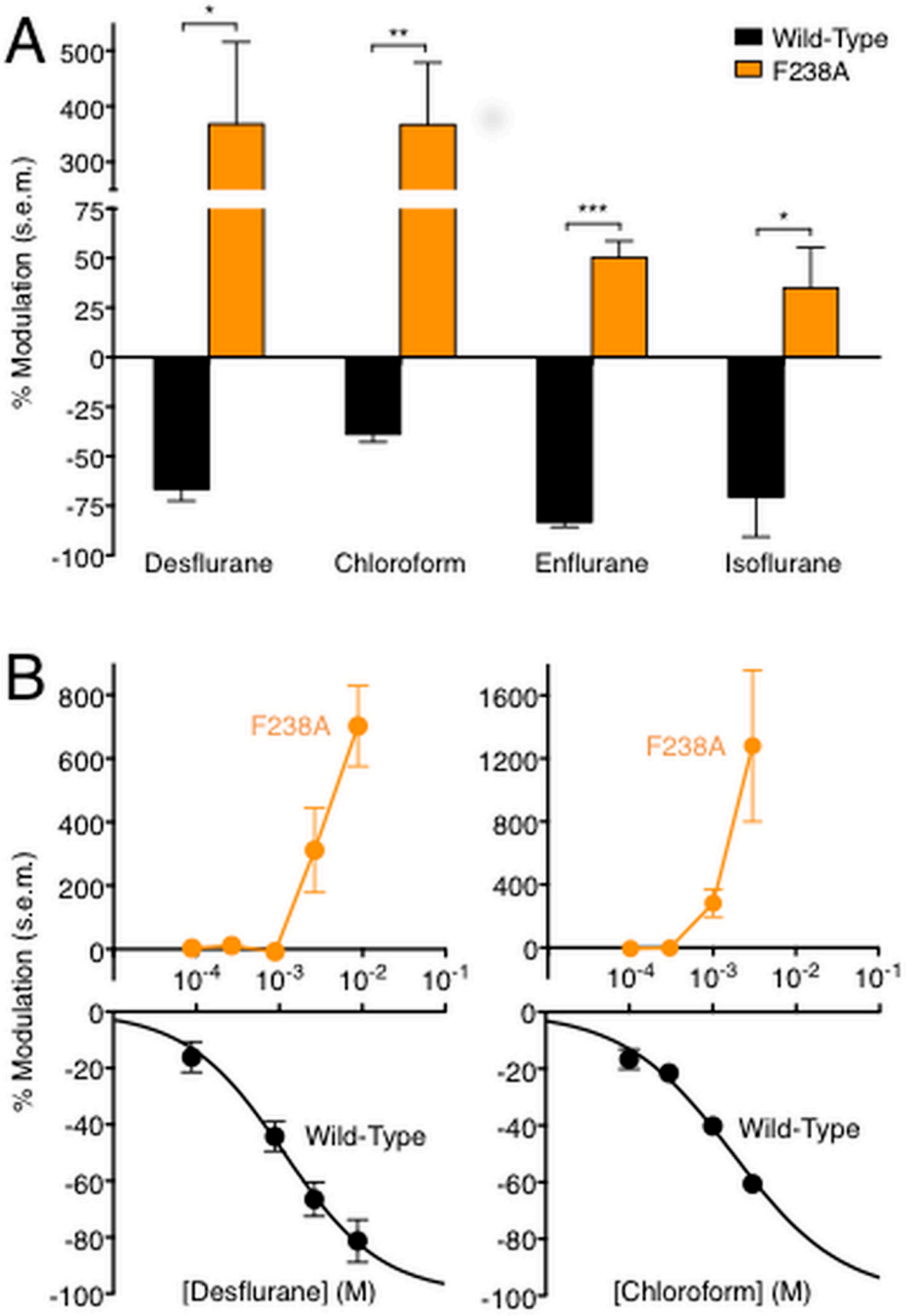

Figure 1.

Enhancement of GLIC potentiation in the F238A mutant. (A) Modulation of GLIC WT (black) and F238A (orange) channels by volatile anesthetics: 1.00 mM chloroform, 2.64 mM desflurane, 1.68 mM enflurane, 0.90 mM isoflurane (significance vs. WT, unpaired *t* test, $*p < 0.05$; $**p < 0.01$; $***p < 0.001$.) Vertical axis is broken to display both WT and mutant responses clearly. Errors are s.e.m., $n = 3–10$. (B) Concentration-dependent modulation of GLIC wild-type (black, lower panel) and F238A (orange, upper panel) channels by desflurane. Black curve represents nonlinear regression fit of WT data; orange lines connect F238A mutant data points, which were poorly fit by regression analysis. Positive and

negative vertical axes are scaled independently to display WT and mutant responses clearly. Errors are s.e.m., $n = 3–14$.

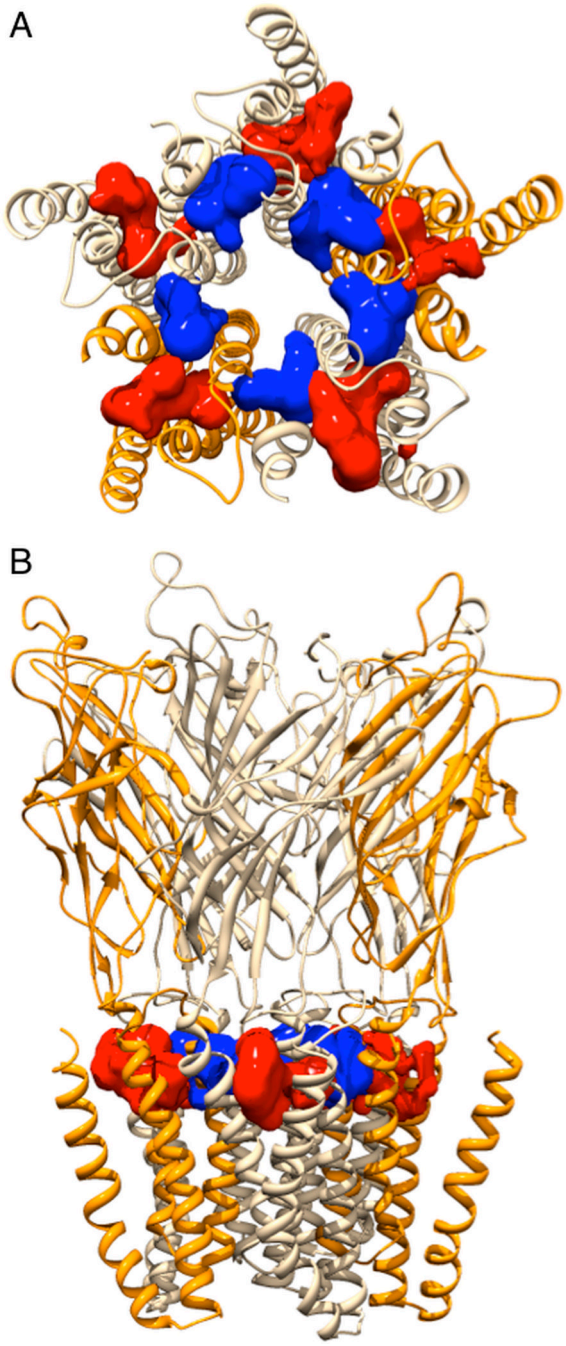

Figure 2.
GLIC F238A TM cavities. Illustration of the intra-subunit (red) and inter-subunit (blue) cavities after equilibration of GLIC F238A, showed from (A) the extracellular side and (B) in the membrane plane. The five subunits are rendered in slightly different colors to visualize the cavity locations. Cavities were calculated and illustrated using the Surfnet module (Laskowski, 1995) in the Chimera program (Pettersen et al., 2004).

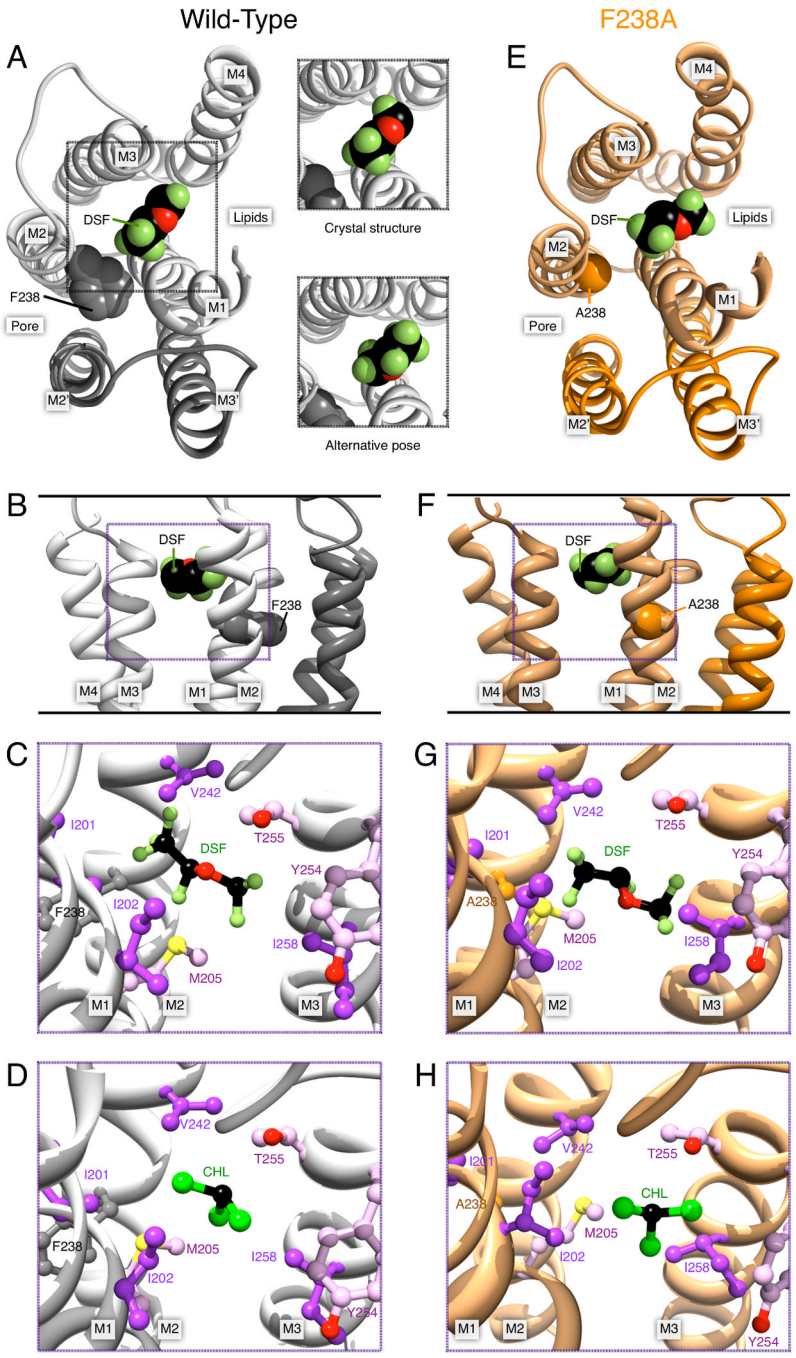

Figure 3.

Desflurane (DSF) and chloroform (CHL) poses in the intra-subunit cavity of GLIC. (A) *Left*, desflurane in the intra-subunit binding site, viewed from the extracellular side. For clarity, only the TM helices M1–M4 of the proximal subunit (light gray) and M2–M3 the distal subunit (dark gray) are shown. Residue F238 (spheres) and helices contributing to the intra-subunit cavity are labeled. *Right*, equivalent view from the extracellular side and a second kinetically distinct pose. (B) Desflurane binding in WT viewed in the plane of the membrane in the pore, with F238 marked. (C) Other important residues surrounding the binding site after equilibration, and (D) residue environment with chloroform (CHL) bound. Panels (E) through (H) illustrate equivalent binding conformations in the F238A mutant,

with residue F238A marked. Overall, the intra-subunit binding was largely unaffected by the mutation.

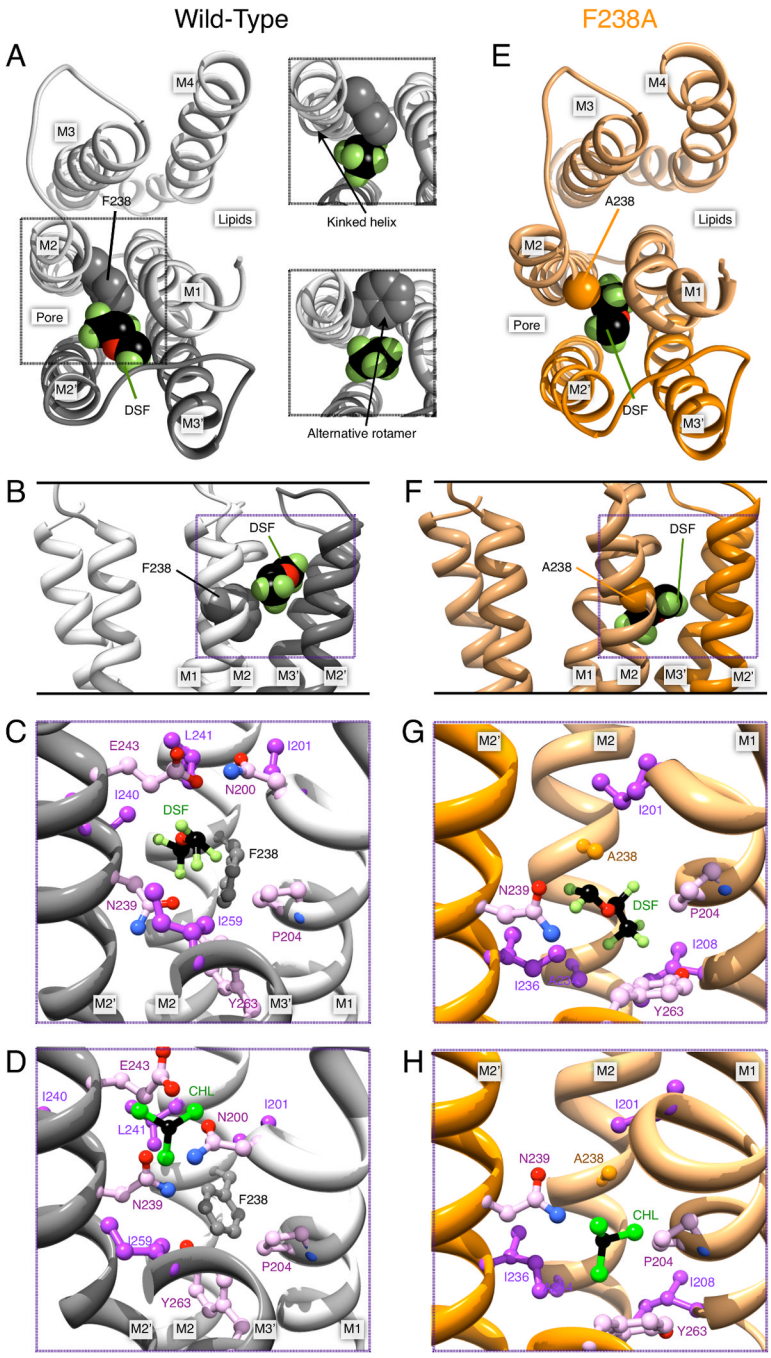

Figure 4.

Desflurane (DSF) and chloroform (CHL) poses in the inter-subunit cavity of GLIC. (A) *Left*, GLIC structure with desflurane in the inter-subunit binding site, viewed from the extracellular side. For clarity, only M1–M4 of the upper subunit (light gray) and M2–M3 from the lower subunit (dark gray) are shown. F238 and helices contributing to the intra-subunit cavity are labeled. *Right*, forcing the ligand to bind in the WT close to F238 either induces a kink in M2, or requires F238 to adopt a different rotamer. (B) Desflurane binding viewed in the plane of the membrane in the pore. (C) Inter-subunit environment for desflurane binding in WT GLIC; note the close proximity to F238. (D) Chloroform bound to the inter-subunit site of WT GLIC. Panels (E) through (H) contain corresponding

illustrations for ligands bound to GLIC F238A. The mutation yields a much larger cavity for ligand binding between the subunits. In particular, in panels (G) and (H), desflurane and chloroform assume poses that would directly overlap with the F238 side chain.

Figure 5.

Free energy of intra-vs. inter-subunit binding. Calculated affinities for GLIC WT (black) and F238A (orange) for desflurane and chloroform in both cavities (Tab. S2). Standard error estimates for the free energy calculation (see supplementary methods) are indicated; $^{**}p < 0.01$. Both ligands preferred intra-subunit binding in WT GLIC, but shift to primarily inter-subunit binding in F238A. This correlates well with the functional results in Fig. 1, and appears to suggest the intra-subunit binding site is primarily inhibitory while the inter-subunit site is potentiating.